Experimental Investigation into Rockfill Dam Failure Initiation by Overtopping

Nasrin Javadi and Tew-Fik Mahdi*

Département des génies civil, géologique et des mines
Polytechnique Montreal
C.P. 6079, Succ. Centreville,
Montréal, Québec, Canada, H3C 3A7.
* Corresponding author: tewfik.mahdi@polymtl.ca , Tel: (514) 340-4711 ext. 5874

Abstract

Rockfill is the most abundant building material. It is often used for water retention under different contexts, such as dams, embankments or drainage systems. Climate change may cause water levels to rise in reservoirs. As rockfill structures are not able to resist strong overtopping flow, rising water levels will constitute a danger for rockfill dam stability as well as for people living nearby. This work is aimed at the development of an empirical formula that enables calculation of the critical water level of overflow at the crest from the geometrical and physical parameters of a dam.

To achieve these objectives, several experimental tests on a rockfill dam model with two different impervious cores, moraine with a sand filter and an empty wooden formwork, were conducted in a hydraulic channel at the hydro-environmental laboratory at École Polytechnique de Montréal. The purpose of these tests was to study the initiation of a riprap failure under the influence of different variables, such as rock size, riprap bank, downstream side slope and bed slope. Results showed linear trends between the critical water level and both the downstream side slope and bed slope. Also, a power trend was observed between the critical level and riprap grain size. A formula that gives the critical overtopping water level was developed from these results.

Keywords

Laboratory tests, Initiation of dam failure, Overtopping level, Critical hydraulic gradient

List of symbols

C_u	Uniformity coefficient (-)
D_{cr}	Critical overflow height (L)
D_{50}	Diameter of the sieve allowing 50% of soil to pass (L)
g	Acceleration caused by gravity (L/T²)

Q		Discharge (L^3/T)
h		Water level (L)
H		Height of the dam (L)
H_n		Height of the core (L)
h_{cr}		Critical water level in the tank (L)
K		Hydraulic conductivity of the soil (L/T)
i_{eff}		Effective gradient (-)
L		Length of the foot of the dam (L)
n		Porosity of sediments (-)
u*		Shear velocity (-)
V		Flow velocity (L/T)
W		Length of the dam crest (L)
W_n		Length of the dam core (L)
α		Empirical exponent (-)
	or	Downstream face angle of the dam (º)
α'		Downstream face angle of the core (º)
β		Upstream face angle of the dam (º)
β'		Upstream face angle of the core (º)
θ		Bed slope angle (º)
ρ		Fluid density (M/L^3)
ρ_s		Grain density (M/L^3)
τ*		Shear stress, Shields parameter (-)

1 Introduction

For many climatological stations in Quebec, the increase in winter temperatures has resulted in an increase in the frequency of freeze-thaw cycles. These episodes, during which temperatures pass the freezing point and remain for some time above 0'C, can have significant impact on the change in the water level upstream of dams and other retaining structures (Milly et al. 2002; Yongpink et al. 2004; Tie and Tang 2009). These may increase the risk of extreme floods that pass over the design of the structures and also increase the risk of ruptured structures caused by overflow. Ralston (1987) has already reported more than 57,000 dams that have the potential for overflow in the United States.

In Quebec, the law on dam safety requires that the crest of a dam that is susceptible to erosion at its lowest point be at least 1 meter above the flood safety level, unless the owner demonstrates to the satisfaction of the department that all hydrologic and hydraulic uncertainties and flood management uncertainties are taken into account when establishing the flood safety height (Assemblée Nationale du Québec 2000).

The rupture of a structure is understood to be the destruction or the movement of a portion of the structure, its support or its foundations, rendering it unable to retain water (Marche 2008). The observation of crumbling embankments has shown different modes of destruction. The most

frequent are breaks from overflow, erosion of the crest and downstream face, or internal erosion of the structure or its foundation. The destruction of a backfill structure by an overflow creates a flood over the crest and erosion resulting from the strength of the current at the foot of the dam, followed by internal erosion of the structure and foundation of the dam, causing the reservoir to empty. This flood then spreads downstream, filling the valley and endangering the lives of inhabitants (Marche 2008). The Commission Internale des Grands Barrages (1994) has demonstrated that around a third of all breaks in backfill dams have been caused by insufficient holding capacity resulting in an overflow over the crest.

According to Goubet (1979), embankments often endure splits before breaking, due to the high permeability of a layer of rock that, during flooding periods, allows excess water to pass through or over the works up to a certain ma38+ximum height without causing the structure to collapse. According to the work of Von Thun and Gilette (1990), a breach in a dam does not necessarily occur when water passes over the crest. Depending on the properties of the fill material, the structure can more or less tolerate overflow over its crest for a long time.

This work presents experimental studies that have dealt with different aspects of three types of rockfill dams breaking: homogenous rockfill dams, rockfill dams that are naturally formed by valleys and rockfill dams with a core. Many studies describe the geometry and development of abreach as well as a hydrograph of homogenous rockfill dams breaking (MacDonald and Langridge-Monopolis 1984; Froehlich 1987; Singh and Scarlatos 1988; Rozov 2003; Chinnarasri et al. 2004; Zerrouk and Marche 2005; Froehlich 2008; Macchione and Rino 2008).Some physical experiments are not able to fully reveal the physical mechanism of flooding because of their relatively small scale (Coleman et al. 2002; Schmocker et Hager 2009). According to Leps (1973), the stability of a homogenous downstream facing rockfill dam depends on the relative density of the material of the dam, the maximum flow rate of infiltration and the inclination of the downstream face of the dam. Franca and Almeida (2004) presented the RoDaB model to calculate the hydrograph resulting from the rupture of a homogenous rockfill dam. They used laboratory experiments to characterize some phenomenological aspects for which, at this time, no analytical approximation exists (a coefficient and an exponent of erosion depends on the material used in the dam). In addition, they carried out a comparison of the model with results from the BREACH model (Fread 1984). This comparison reveals that the potential failure of a rockfill dam is minor compared to that of an earth dam and it will collapse in a different manner.

A series of tests conducted by Liao and Chou (2003) was specifically focused on understanding the different mechanisms of failure of rockfill dams that are naturally formed in valleys by landslides. For experimental purposes, a dam with a large crest length and a variable slope between 12° and 24° was placed in a channel. Gregoretti et al. (2010) have worked to improve the understanding of hydraulic and sedimentological conditions that lead to flooding and erosion of the crest of rockfill dams that are naturally formed. To do this, they carried out a systematic series of experiments for different configurations of the dam, as well as a wide range of grain sizes and bed slopes. The experimental results were used to determine a dimensional relationship

between the critical water level of the reservoir and the available parameters such the channel bed slope, several geometrical parameters characterizing the configuration of the dam, and the physical properties of the material. According to their results, the critical water level reaches the maximum peak of the dam.

This review found that the focus of previous work has been placed on geometry and the development of a breach, on the hydrogram of the rupture and the stability of the downstream slope. Little work has been done on models of a dam with a core. In addition, no study has been found that is focused on the prediction of the initiation of the breach of a rockfill dam with a core caused by the overflow of water over the crest using the geometrical parameters of the dam.

In the present work, we aim to improve the understanding of hydraulic and sedimentological conditions that lead to the rupture of a dam because embankments are generally not capable of withstanding strong outbursts. The overall objective in this research is to study the initiation of the breakdown of the top layer of rock (charging) of a zoned embankment caused by the overflow of water over the crest of the dam. The specific objective was to visually predict the position of the start of erosion at the downstream face of the dam, which causes the beginning of the movement of rock, and also to find an empirical relationship to determine the critical height of the overflow that causes the initiation in the rupture by using a dimensional analysis. This empirical relationship has the advantage of relying solely on geometrical parameters, which makes it simple and practical. To do this, we performed multiple tests on laboratory scale models of the hydro-environment at École Polytechnique de Montréal in order to determine the critical height of the overflow over the crest of the dam that causes the initiation of the rupture as a result of different parameters such as particle size, the slope of the downstream face and the slope of the bed.

This article contains four sections. The first section introduces the topic, presents the existing problems and the objectives and overview of previous work. The second section details the experimental and physical properties of the materials used, as well as highlights the experimental process of testing and the sensitivity analysis of different parameters. The third section illustrates the experimental results followed by an analysis to emphasize the shape of the empirical relationship representing the results. The final section concludes and makes recommendations for future research.

2 Experimental study

2.1 Apparatus and materials

The diagram in Figure 1 illustrates the configuration of the experimental setup. The dam was built in a rectangular channel with a 14.8 m length, 0.5 m depth and 0.76 m width. At the dam level, the wall of the channel is in glass, which allows for observation of the flow through the dam and the movement of particles. The length of the channel allows the formation of a holding

tank of 5.7 m³. Four ultrasonic sensors were used in the tests. The sensors were placed in the center of the channel to avoid walls' influence on the reading of water levels. The use of these ultrasonic sensors allows a measurement to be taken without water contact, which provides the advantage of not disturbing the flow.

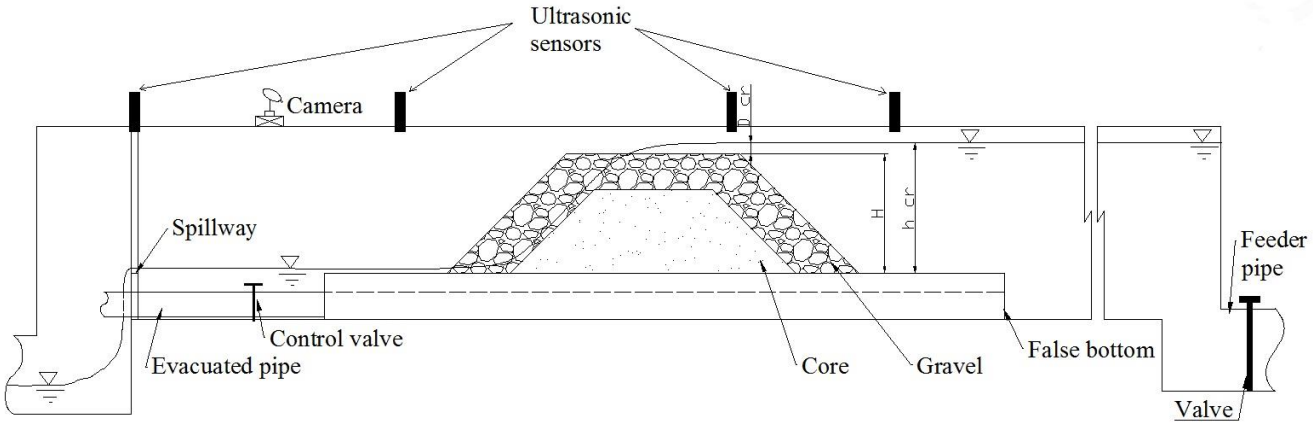

Figure 1: Diagram of the experimental setup

In its entirety, the dam spans the width of the channel. The crest length and base length were set at 63 cm and 149 cm, respectively. The height was 43 cm. The upstream slope was set to 1V: 1H, while the downstream varied for the sensitivity analysis.

Two apparatuses have been studied in the choice of an impervious core in the dam: the first was with moraine and sand and the second with an empty wooden formwork. The rip rap, sand diameters and the geometrical dimensions are the same as those of Maknoon and Mahdi (2010).

- *Dam with watertight soil core*

The core consists of clay and sand moraine. The core has dimensions of 33 cm crest length, 63 cm base length and 15 cm height. Each slope, upstream and downstream, are formed at a 45° angle. The filter layer, placed over the core, has a thickness of 15 cm and a length of 43 cm at the peak and 103 cm at the base. The inclination of the two faces is the same as that of the core. The gravel bed has a length of 63 cm at the peak, with a thickness of 13 cm. The slope of the upstream face is fixed at 45°, while the downstream slope varies for different tests. Figure 2 illustrates the typical cross-section of this model.

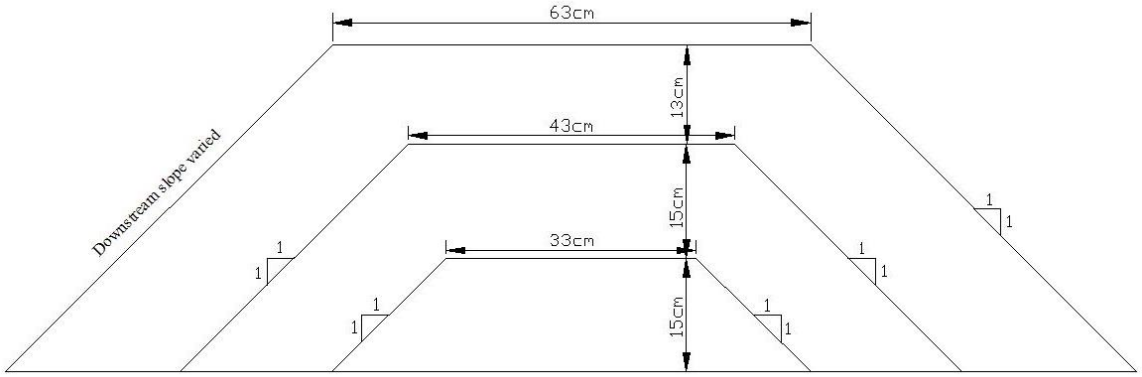

Figure 2: Cross section of the dam made with a soil core

- *Dam with a sealed wooden core*

The core was replaced by an empty wooden formwork. Its dimensions are those of the external bounds of the sand (filter) layer, 43 cm length at the peak and 103 cm length at the base, with 30 cm height. The wooden formwork was sealed well and its location was fixed with silicone along the sides of the channel. The gravel layer has the same dimensions as those present in the dam with the earth core. A diagram of the dam is illustrated in Figure 3.

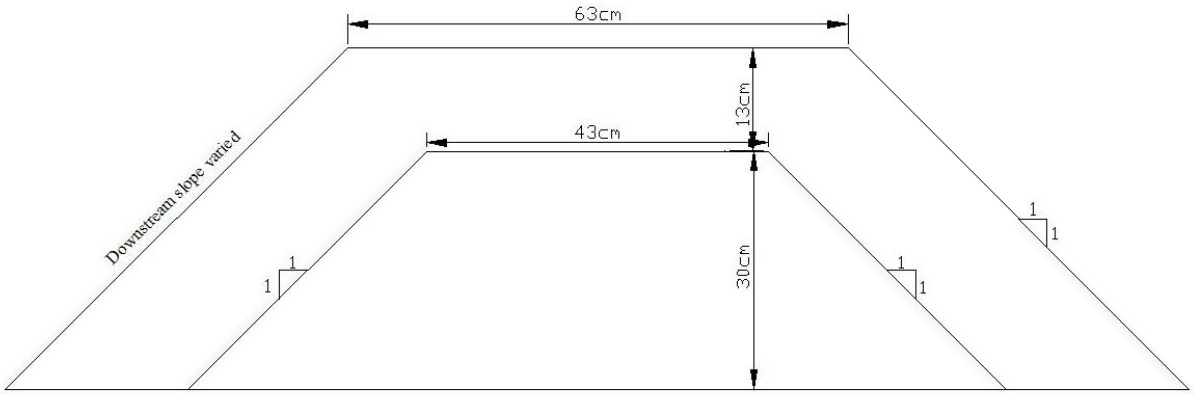

Figure 3: Cross section of the dam that contains a wooden core

Regarding the materials used, gravel in three different sizes was chosen for the outer layer: 10-14mm, 14-20 mm and 20-25 mm. Moraine was used to seal the model. The sand acted as a filter between the core and the top layer of gravel. To ensure that the materials met the placement requirements, some of their properties such as particle size, relative density, degree of compaction and permeability were examined (Table 1).

Table 1: Properties of the material used

Sand	Moraine	Gravel 10-14 mm	Gravel 14-20 mm	Gravel 20-25mm

Optimal water content (%)	5.0	10.8	-	-	-
Maximum dry density (kg/m³)	1867	1892	-	-	-
Hydraulic conductivity, K (cm/s)	7.46E-03	4.52E-04	-	-	-
Porosity – according to compaction test	0.323	0.301	-	-	-
Porosity – in the column	-	-	0.417	0.420	0.440
Porosity – in the dam	-	-	0.393	0.395	0.396
Relative density	2.73	2.70	2.69	2.71	2.74
Diameter of the sand, 50% passing through, D_{50} (mm)	1.60	0.18	11.96	16.67	21.95
Uniformity index, C_u	5.94	2.83	1.20	1.19	1.20

2.2 Execution of the test

Experiments on different geometries and compositions of dams were conducted to study the beginning of the breach in the layer of the charge. The following sections detail the experimental protocol.

2.2.1 Preparation of material and dam setup

The first series of tests was carried out following the construction of a dam consisting of a core and a filter in the ground. In the second series of tests, a wooden formwork replaced the core and filter.

For each model, the predefined dimensions of the layers were marked on the outside of the side wall windows along the channel, to base the construction of the dam upon (Figure 4).

Figure 4: Marks on the glass walls of the channel of the dimensions of the layers

The moraine and sand were placed one layer at a time, each with a thickness of several centimeters, and compressed by the dead weight of a mechanical hammer by 93% ±2% and 92% ± 2% degree of compaction, respectively for the layer of moraine and sand. After placing the core and the filter, the rock layer was placed over the main body of the dam.

In the second model of the dam, the wooden casing was set in the channel with silicone. Once the silicone was thoroughly dried, the next step was to lay the gravel layer. The gravel was placed on top of the casing as it had been in the soil core model.

2.2.2 Test procedure

To begin, the channel was fed by a constant flow of intake and the water level was regulated at a constant level over the crest of the filter for three days to allow the moraine and sand become saturated to obtain maximum hydraulic conductivity as well as maximum filtration output.

The initial condition of the test was characterized by a constant flow of intake, Q_0. To minimize the relative error on the critical height of the water that causes the initiation of a breach on the downstream face, the flow rate was increased in small increments of 3×10^{-4} m^3/s, resulting in increased depth of water of 2×10^{-3} m. At each increment of the flow, 10 to 15 minutes was required to stabilize the water level before beginning the measurements. Once the flow is equal to Q_0, we observe a thin blade at the foot of the downstream face as a result of infiltration into the layer of sand. Once the flow rate increased, the water level crossed the sand/gravel interface and we began to observe flow in the gravel level. The impact of this increase in the water level on the stability of the downstream face depends on the size of the ripraps and the geometry of the dam. Once the upstream water level exceeds the critical value, the flow at the foot of the downstream face begins to erode particles. By gradually increasing the flow as illustrated in Figure 5, the flow carries the particles at the bottom of the downstream face (it should be noted that while we were in this phase, the structure remained stable and held its ability to retain water upstream); next, the erosion spreads up the sides, forming a breach. The test was terminated before reaching the final breach.

Figure 5: Phase beginning the breach at the foot of the downstream face

During the tests, the load of the tank and the charges at the entrance and the exit of the dam were recorded by ultrasonic sensors. Note that when the water is inside the dam, a measuring tape stuck on the glass showed water levels upstream of the crest, whereas levels were recorded by ultrasonic sensor when the overflow occurred.

2.2.3 Sensitivity study

The inability to analytically predict the time a breach begins from physical and geometric parameters of a dam is mitigated by experimental approaches. The objective is to correlate, in a direct relationship, the critical level in a reservoir causing the initiation of a breach, and the physical and geometrical parameters of a dam.

First of all, it is important to develop the parameters that play an important role in the instability of a dam and the formation of the breach. The parameters affecting the rupture of the dams are overflow liquid properties (such as density and viscosity), the flow conditions (such as the flow rate and the upstream water level), and the material properties forming the dam such as permeability, shape and particle size distribution (Zhao 1992). Local sediment stability and its ability to be transported generally depends on several factors such as the properties of the fluid and sediment, the water depth and the shear velocity (u_*).The determination of the shear stress (the counterpart dimension, the Shields Parameter, τ_*) requires knowledge of quantities that are difficult to estimate, such as the flow of the infiltration output (Gregoretti, Maltauro et al. 2010). Rather than focusing on the local mobility of particles, the overall stability of the system was connected to the overall geometrical and physical parameters of the structure. To characterize the critical water level overflow over the crest, D_{cr}, it was proposed to use parameters that define the overall stability, such as the following: ρ, ρ_s, d_{50}, g, L, H, W, H_n, W_n, $\tan\alpha$, $\tan\beta$, $\tan\alpha'$, $\tan\beta'$, $\tan\theta$, n, K.

Following the dimensional analysis, only three variables of particle size distribution, slope of the downstream face and slope of the bed, were made in the study.

- *Particle size distribution*

The size of the rock was one of the studied parameters. Three sizes of rock for the composition of the backfill layer were selected: 10 to 14 mm, 14 to 20 mm and 20 to 25 mm. When studying the influence of different sizes of granules, the slope of the downstream face and the bed of the selected horizontal channel were set at 45 degrees.

- *Slope of the downstream face*

In order to analyze the influence of the slope on the initiation of the breach, different slope values were tested: 45, 40, 35 and 30 degrees. For tests that had a variation in the slope of the downstream face, the particle size distribution of 14-20 mm and a horizontal channel bed were chosen.

- *Slope of the bed*

A wooden board, placed at the desired angle, produces different bed slopes. The slopes considered are inclines of 0, 1.5, 3 and 5 degrees. The particle size distribution of 14-20 mm and a 45 degree slope of the downstream face were selected for this study. These sensitivity studies were conducted to achieve 12 different types of tests, summarized in Table 2: Tests conducted

Test number	Main material of the body		Variable studied			
	Material	d50 (mm)	Backfill material		Bed slope, α (degrees)	Downstream slope, θ (degrees)
			Material	d50 (mm)		
1	Moraine/Sand	0.18 / 1.6	Gravel	11.96	0	45
2	Moraine/ Sand	0.18 / 1.7	Gravel	16.68	0	45
3	Moraine/ Sand	0.18 / 1.6	Gravel	21.95	0	45
4	Wood formwork	-	Gravel	11.96	0	45
5	Wood formwork	-	Gravel	16.68	0	45
6	Wood formwork	-	Gravel	21.95	0	45
7	Wood formwork	-	Gravel	16.68	1.5	45
8	Wood formwork	-	Gravel	16.68	3	45
9	Wood formwork	-	Gravel	16.68	5	45
10	Wood formwork	-	Gravel	16.68	0	40
11	Wood formwork	-	Gravel	16.68	0	35
12	Wood formwork	-	Gravel	16.68	0	30

.

Table 2: Tests conducted

Test number	Main material of the body		Variable studied			
	Material	d_{50} (mm)	Backfill material		Bed slope, α (degrees)	Downstream slope, θ (degrees)
			Material	d_{50} (mm)		
1	Moraine/Sand	0.18 / 1.6	Gravel	11.96	0	45
2	Moraine/ Sand	0.18 / 1.7	Gravel	16.68	0	45
3	Moraine/ Sand	0.18 / 1.6	Gravel	21.95	0	45
4	Wood formwork	-	Gravel	11.96	0	45
5	Wood formwork	-	Gravel	16.68	0	45
6	Wood formwork	-	Gravel	21.95	0	45
7	Wood formwork	-	Gravel	16.68	1.5	45
8	Wood formwork	-	Gravel	16.68	3	45
9	Wood formwork	-	Gravel	16.68	5	45
10	Wood formwork	-	Gravel	16.68	0	40
11	Wood formwork	-	Gravel	16.68	0	35
12	Wood formwork	-	Gravel	16.68	0	30

3 Results and discussion

The tests on the rockfill dam model with a tight core were used to study the threshold level of water flowing over the crest of the dam, causing the beginning of the breach on the downstream face. Once the central zone was sealed, the passage of water through the body of the embankment is made in the layer of gravel. The initiation of the breach took form at a given place and it was of great interest to locate the critical point in order to calculate the losses that generated the break at that point. The focal point of the flow at the exit of the dam was located at the base of the downstream face. The increase in flow rate was done gradually and caused a thickening of the depth at the exit point, as well as caused the erosion of stone at the foot of the downstream base. This has been identified as the critical position, because the increased flow caused particles to be washed out following a slip in the siding materials.

3.1.1 Analysis of the critical gradient

The effective hydraulic gradient through, i_{eff}, the dam was evaluated in order to ascertain the losses between the input and the critical position at the exit of the dam.

$$i_{eff} = \frac{\Delta h}{\Delta x} \quad (1)$$

With:

Δh : head difference between the two measurement points

Δx : horizontal distance between the two measurement points

The evolution of the effective gradient in function of the flow rate has been plotted for the purpose of illustrating the increase in gradient, to the point of inflection, i_{effc}, which is associated with the critical water level (initiation of the breach), from which there is a decrease in the gradient while the flow continues to increase. Figure 6 illustrates this procedure for the tests on the sensitivity of the particle size (a trial for each category is presented). The evolution of the curves shows a gradual increase in the flow rate and the effective gradient. Once the rupture initiates, following the gradual erosion at the foot of the dam, this causes a decrease in the gradient. Since the dam maintains its resistance for some time after the initiation of the breach, the decrease in the gradient is very slow (additionally, the ripraps are large in size, or the downstream side and bed slopes are softer, and the final formation of the breach is slowed). The increases in the flow causing landslides of the slopes explain small ruptures on the bends.

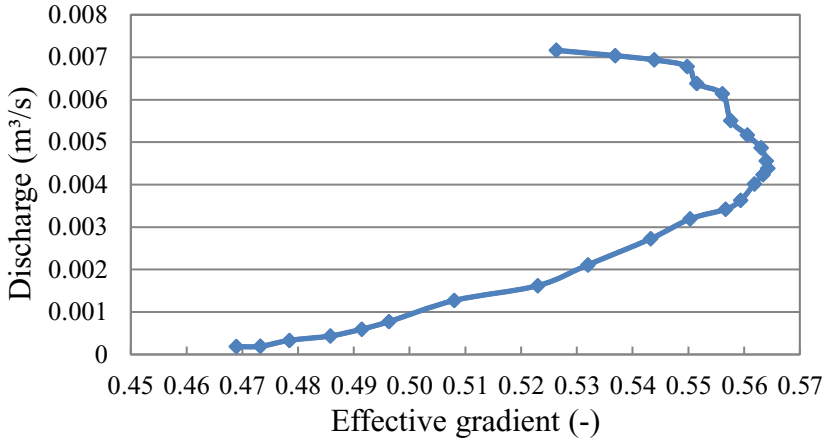

a)

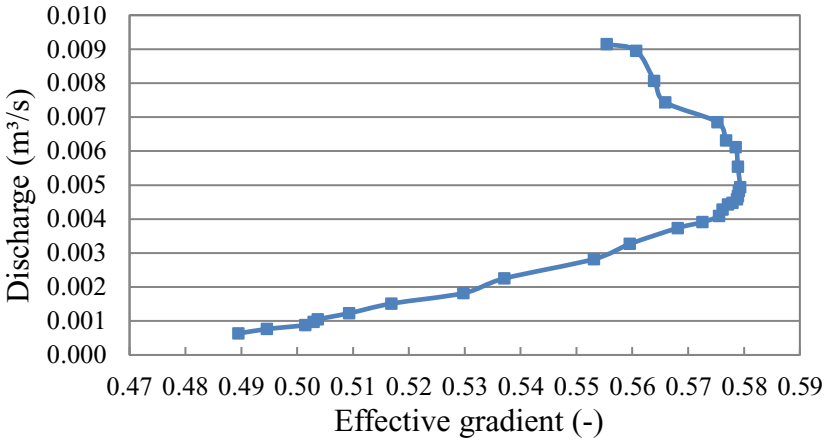

b)

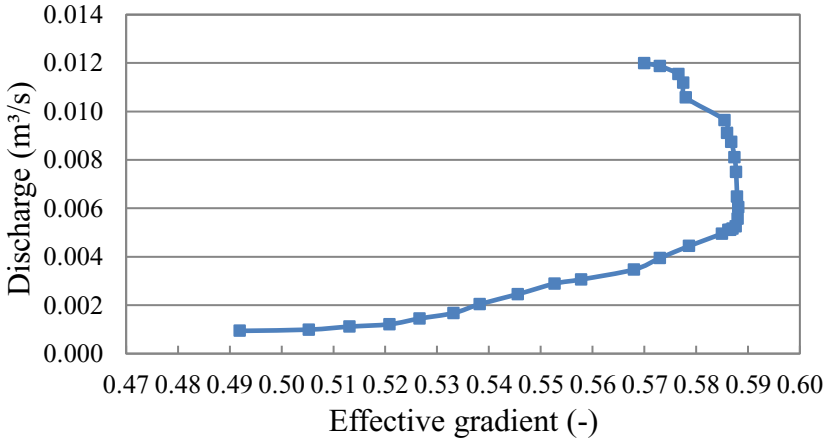

c)

Figure 6: Change of the effective gradient as a function of the flow rate on a dam with a wooden formwork a) 10-14 mm gravel with $\alpha = 45^{o}$ and $\theta = 0^{o}$ b) 14-20 mm gravel with $\alpha = 45^{o}$ and $\theta = 0^{o}$ and c) 20-25 mm gravel with $\alpha = 45^{o}$ and $\theta = 0^{o}$

The shape of the curve is essentially the same from one test to another for each variant. Small differences in results exist at each flow change, but it is possible that the variations in the flow are not exactly the same because the opening of valves was done manually.

By comparing the results obtained from testing the model with the dam made of a soil core and the model of the dam with a wooden frame, it was concluded that the gap starts at the same upstream water level. However, there is an increase in the water level at the output of the dam of one centimeter maximum in length at the beginning of the breach in the instance of the soil core, which corresponds to the decrease of the gradient. Figure 7 presents the results of the critical point of these tests. According to the calculation of the maximum infiltration rate through the entire core and filter, a flow rate of 2×10^{-6} m³/s was obtained. Since the infiltration is negligible based on the hypothesis of the existence of a proper seal in the dam, it was decided to replace the earth core with a wooden formwork for the remainder of the tests. The form directly conducted the water towards the most permeable layer, the gravel, eliminating the need to retouch the filter during the application of gravel during each test, and facilitating the reconstruction of the dam during a study of the sensitivity of the slope of the bed.

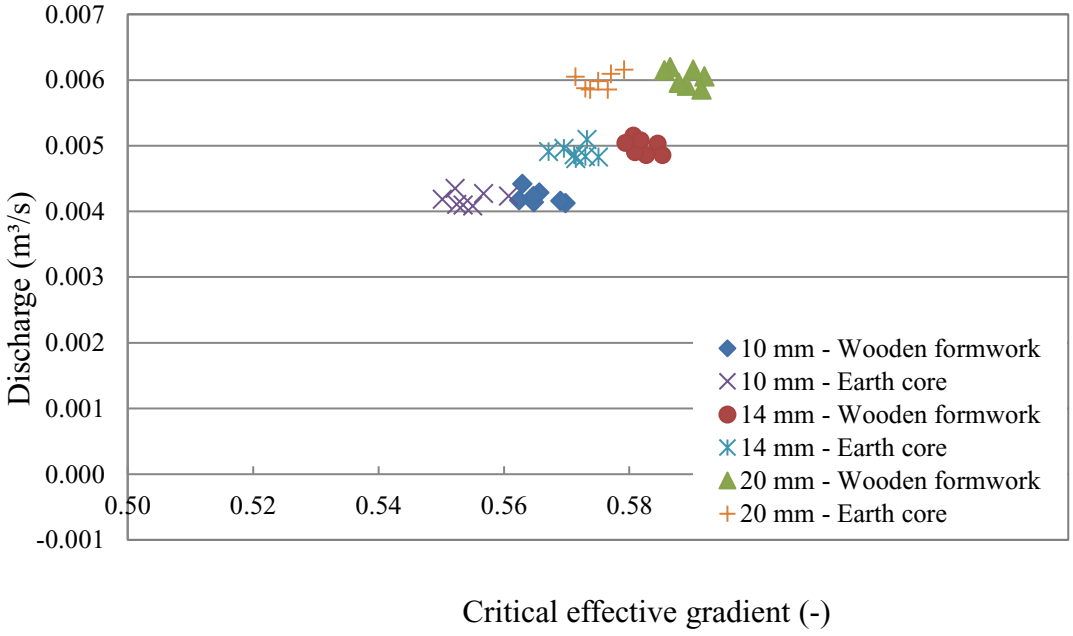

Figure 7: Comparison of the gradient that is critical to the initiation of the breach for two core types: soil and wood formwork

3.1.2 Critical water height over the crest

The results of three sensitivity tests on the initiation of the breach in the dam correspond to the critical water overflow height over the crest of the dam in a dimensionless form. For each sensitivity analysis, six to seven successive tests were run on the same model to ensure consistent results. The critical water level in the tank, h_{cr}, is associated with the critical gradient, $i_{eff\,c}$, corresponding to the critical flow rate. The difference between the critical water level in the tank and the elevation of the crest of the dam, the critical height of the overflow, D_{cr}, was calculated.

The size of the ripraps, represented by d_{50}, was the first variable in the study. The level of the reservoir was obtained by the particle sizes of 20-25 mm and was 3 cm above the crest. Using the best curve and applying the method of least squares on the result of the critical water level of the overflow, a power curve shape ($y = a + bx^c$) fits the measured data well with a regression coefficient of 0.955 (Figure 8a). The second variable of interest was the slope of the downstream face, α. This is what allowed for the highest levels of water for the gentlest slopes. A linear form curve ($y = a + bx$) is consistent with the results obtained with a regression coefficient of 0.924 (Figure 8b). The third variable studied was the influence of the bed slope, θ, on the critical water height of the overflow. As with the slope of the downstream face, a linear curve ($y = a + bx$) was adjusted to the measured data for a regression coefficient of 0.982 (Figure 8c).

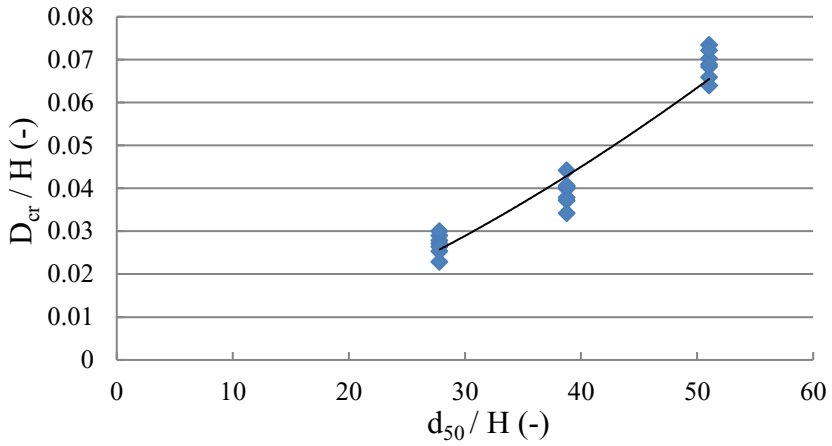

a)

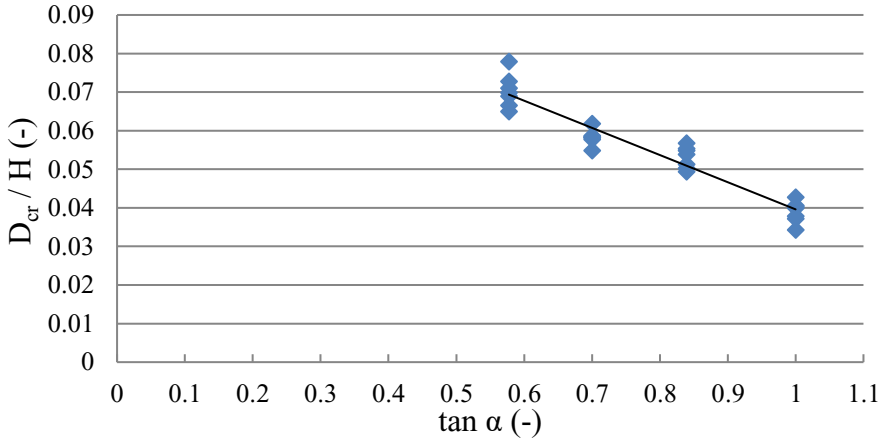

b)

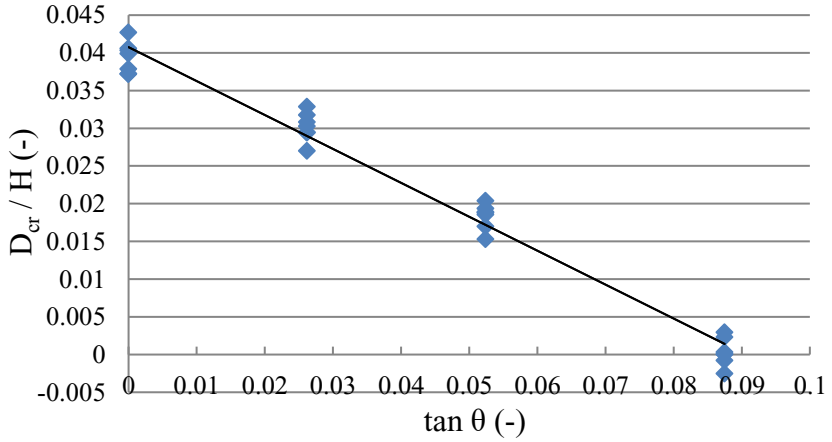

c)

Figure 8: Dimensionless critical water heights over the crest under the effect of different variables a) particle size b) the downstream slope and c) the slope of the bed.

3.2 Development of the regression curve

For a multivariate analysis, it was possible to connect all variations of the four variables. The objective was to present a practical empirical relationship for the critical height of the overflow, in function of other variables that are easier to obtain, such as the slope of the downstream face, the size of the particles and the slope of the bed. To do this, using the general regression of each variable depending on the dimensionless height of the critical water overflow, the form suggested by Gregoretti et al. (2010) was used:

$$\frac{D_{cr}}{H} = \left[a + b\tan\theta\right]\left[c + d\left(\frac{d_{50}}{H}\right)^{g}\right]\left[e + f\tan\alpha\right] \quad (2)$$

The coefficients a, b, c, d, e, f and g of the empirical formula (2) were determined by minimizing the sum of the square differences between measured values and those that were calculated. The following values were obtained: a= 0.0391, b = -0.4446, c = 0.1299, d = 0.4173, e = 0.3931, f = -0.2042 et g = 0.7247.

Equation 3 is therefore the relationship between the critical height overflow with the variables involved in the test conditions.

$$\frac{D_{cr}}{H} = \left[0.0391 - 0.4446\tan\theta\right]\left[0.1299 + 0.4173\left(\frac{d_{50}}{H}\right)^{0.7247}\right]\left[0.3931 - 0.2042\tan\alpha\right] \quad (3)$$

The points shown in Figure 9 are the result of eleven experiments on eight geometries and three different sizes of gravel. Looking at the graph reveals a match between the empirically calculated values and the experimentally measured values. This is confirmed by the perfect fit line ($y = x$), in which all the values found experimentally coincide with the results of the empirical formula that was developed. The correlation coefficient for the best fit is 0.96. All items, except for five, were situated between the dotted lines, which correspond to the maximum uncertainty of ± 0.0103 in empirically determining D_{cr}/ H.

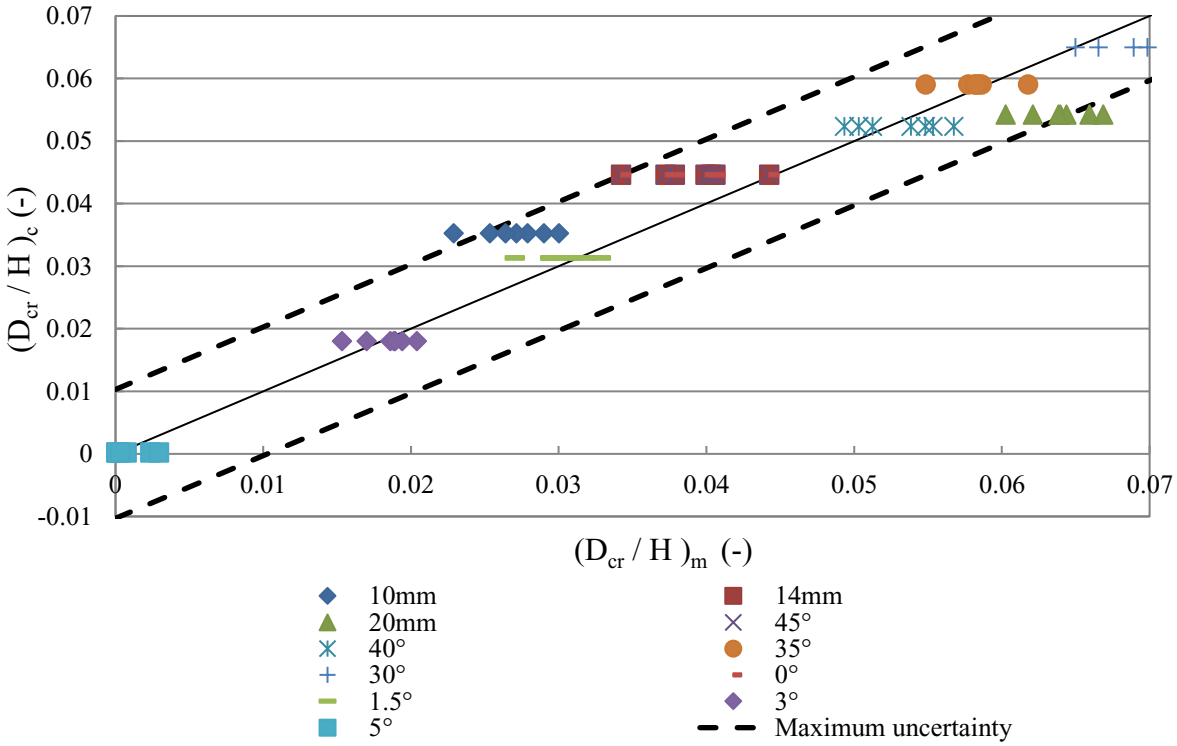

Figure 9: A comparison of the measured dimensionless overflow heights $(D_{cr}/H)_m$ and empirical calculations $(D_{cr}/H)_c$ corresponding to the beginning of the breach.

It should be noted that the relationship developed has limits to its application. In effect, the downstream slope must obey the rules of the stability of the slope: the angle at which the gravel rests is 45°, which must be taken as an upper limit for α. The minimal angle used in the tests is 30° taking into account the constraints of the length of the channel in the experiment; this relationship is not guaranteed below 30° slopes. The angle of inclination of the channel varied between 0° and 5°, which corresponds to a slope between 0 and 8.7%. This interval is representative of natural slopes. The values of d_{50}/H that were used are between 0.023 and 0.046. It is expected that the developed relationship provides better performance in this interval.

The calculation of uncertainty is an important aspect in any laboratory experiment because the inaccuracy of the experimental data can affect the results. The absolute uncertainty of the results based on the one hand, the accuracy of measuring instruments and human factors, and the other, the error propagation on the errors of variables involved. The absolute uncertainty in different amounts directly measured or calculated, is compiled in Table 3. Uncertainty ranges for some calculated amounts are also presented. The uncertainties were determined by the extreme value method for amounts with a linear dependence on a single variable and differential method for equations with more than two variables with uncertainty.

399 Table 3: Absolute uncertainties on some measured and calculated amount

Measured or calculated amount	Units	Absolute uncertainty
Dimensions of the dam	m	± 0.001
Critical overflow height calculated* (Dcr)	m	± 0.0008 – 0.0009
Critical water level in the tank (hcr)	m	± 0.003
Discharge* (Q)	m^3/s	± 0.000018 – 0.000032
Effective gradient (ieff)	-	± 0.0014 – 0.0015
Flow velocity mesured* (V)	m/s	± 0.0005 – 0.0015
Water level (read by ultrasound sensor) (h)	cm	± 0.0165
Water level (visual reading) (h)	m	± 0.001
Height of the dam (H)	m	± 0.004
Downstream face angle of the dam (α)	-	± 0.3
Bed slope angle (θ)	-	± 0.2
Representative diametre (d50)	mm	± 0.05

400 * Uncertainties Obtained by calculating

401 # 4 Conclusion

402 This paper investigates under which conditions a earth dam may fail: presently, the standards
403 used to perform hydraulics safety studies, initiates the breach when the water level reached the
404 dykes top. The experiment described in this paper show that the failure occurs for a water level
405 higher than the dyke's top. An empirical relationship for the critical effective hydraulic gradient
406 is proposed to evaluate the water level at which the breach may initiate. Please note that a delay
407 in the breach formation, compared to standards' recommendations, has a positive impact on dam
408 break flood's time of propagation and hence on the evacuation available time.

409 This work has led to a better understanding and analysis of the mechanisms of a rupture of
410 rockfill dams with an impervious core through the use of an experimental model. Systematic
411 rupture tests of overflow in different geometric and physical configurations of the model were
412 made. These tests considered the position of the foot of the dam as a point of reference for the
413 initiation of the breach, which is practical and physically identifiable in practice. The
414 understanding of this allows for the calculation of an effective gradient that increases gradually
415 and according to the flow rate through the dam until it reaches the critical value, which is the
416 moment of the onset of a rupture. This point indicates the critical water level in the tank.
417 Dispersion points on the graph show that the critical overflow height varies linearly with the
418 downstream slope with that of the bed of the channel, while it varies with a power relationship in
419 the size distribution of the gravel. The effect of this latter parameter on obtaining a high critical
420 water height was more significant than those of the other geometric parameters. By collecting
421 critical water levels of the reservoir in all tests, an empirical relationship has been developed.
422 This approach has the advantage of relying on only four parameters of entry, which are: the
423 height of the dam, the angle of the downstream slope, the angle of the dam bed and the size of
424 the gravel.

References

Assemblée Nationale du Québec (ANQ) (2000). "Loi sur la sécurité des barrages, Projet de loi 93." Publications du Québec.

Chinnarasri, C., S. Jirakitlerd, et al. (2004). "Embankment dam breach and its outflow characteristics." Civil Engineering and Environmental Systems 21(4): 247-264.

Coleman, S. E., D. P. Andrews, et al. (2002). "Overtopping breaching of noncohesive homogeneous embankments." Journal of Hydraulic Engineering 128: 829.

Commission internationale des grands barrages (CIGB) (1994). "Comptes rendus." Congrès international des grands barrages, Paris

Franca, M. and A. Almeida (2004). "A computational model of rockfill dam breaching caused by overtopping (RoDaB)." Journal of Hydraulic Research 42(2): 197-206.

Fread, D. (1984). "A breach erosion model for earthen dams." National Weather Service (NWS) Report, Silver Spring, MA, USA

Froehlich, D. C. (1987). EMBANKMENT-DAM BREACH PARAMETERS. Hydraulic Engineering, Proceedings of the 1987 National Conference., Williamsburg, VA, USA, ASCE.

Froehlich, D. C. (2008). "Embankment Dam Breach Parameters and Their Uncertainties." Journal of Hydraulic Engineering 134(12): 1708-1721.

Goubet, A. (1979). "Risques associés aux barrages." La Houille Blanche(8): 475-490.

Gregoretti, C., A. Maltauro, et al. (2010). "Laboratory Experiments on the Failure of Coarse Homogeneous Sediment Natural Dams on a Sloping Bed." Journal of Hydraulic Engineering 136: 868.

Leps, T. M. (1973). "Flow through rockfill." Embankment-Dam Engineering.

Li, B. and M. H. Davies (1998). "Relationships for non-Darcy flow in rockfill." Journal of Hydraulic Engineering 124: 206.

Liao, W. M. and H. T. Chou (2003). Debris flows generated by seepage failure of landslide dams. 3rd International Conference on Debris-Flow Hazards Mitigation: Mechanics, Prediction, and Assessment, September 10, 2003 - September 12, 2003, Davos, Switzerland, American Society of Civil Engineers.

Macchione, F. and A. Rino (2008). "Model for predicting floods due to earthen dam breaching. II: Comparison with other methods and predictive use." Journal of Hydraulic Engineering 134: 1697.

MacDonald, T. C. and J. Langridge-Monopolis (1984). "Breaching Charateristics of Dam Failures." Journal of Hydraulic Engineering 110: 567.

Maknoon, M. and Mahdi, T.F. (2010). Experimental Investigation Into Embankment External Suffusion. *Natural Hazards, 54(3),* p. 749-763.

Marche, C. (2008). Barrages: crues de rupture et protection civile, Presses inter Polytechnique.

Maknoon M. and T. Mahdi (2010).

Milly, P. C. D., R. T. Wetherald, et al. (2002). "Increasing risk of great floods in a changing climate." Nature 415(6871): 514-517.

Ralston, D. C. (1987). Mechanics of embankment erosion during overflow, ASCE.

Rozov, A. L. (2003). "Modeling of washout of dams." Journal of Hydraulic Research 41(6): 565-577.

Schmocker, L. and W. H. Hager (2009). "Modelling dike breaching due to overtopping." Journal of Hydraulic Research 47(5): 585-597.

Singh, V. P. and P. D. Scarlatos (1988). "Analysis of gradual earth-dam failure." Journal of Hydraulic Engineering 114(1): 21-42.

Tie, Y. B. and C. Tang (2009). "Progress in glacier lake outburst assessment system." Advances in Water Science 20(3).

Von Thun J. L., G. D. R. (1990). "Guidance on Breach Parameters, un published internal document, U. S. Bureau of Reclamation." Denver, Colorado: p.17.

Yongping, S., D. Yongjian, et al. (2004). "An increasing glacial lake outburst flood in the Yarkant River, Karakorum in past ten years." Journal of Glaciology and Geocryology 26(2): 234.

Zerrouk, N. E. and C. Marche (2005). "Une contribution experimentale a l'etude de l'erosion d'une digue par submersion et son analyse." Revue des Sciences de l'Eau 18: 381-401.